Tellus (2006), 58B, 73–87
Printed in Singapore. All rights reserved

TELLUS

The role of Southern Ocean mixing and upwelling in glacial-interglacial atmospheric CO_2 change

By ANDREW J. WATSON* and ALBERTO C. NAVEIRA GARABATO†, *School of Environmental Sciences, University of East Anglia, Norwich NR4 7TJ, United Kingdom*

(Manuscript received 10 February 2005; in final form 12 July 2005)

ABSTRACT

Decreased ventilation of the Southern Ocean in glacial time is implicated in most explanations of lower glacial atmospheric CO_2. Today, the deep (>2000 m) ocean south of the Polar Front is rapidly ventilated from below, with the interaction of deep currents with topography driving high mixing rates well up into the water column. We show from a buoyancy budget that mixing rates are high in all the deep waters of the Southern Ocean. Between the surface and ~2000 m depth, water is upwelled by a residual meridional overturning that is directly linked to buoyancy fluxes through the ocean surface. Combined with the rapid deep mixing, this upwelling serves to return deep water to the surface on a short time scale.

We propose two new mechanisms by which, in glacial time, the deep Southern Ocean may have been more isolated from the surface. Firstly, the deep ocean appears to have been more stratified because of denser bottom water resulting from intense sea ice formation near Antarctica. The greater stratification would have slowed the deep mixing. Secondly, subzero atmospheric temperatures may have meant that the present-day buoyancy flux from the atmosphere to the ocean surface was reduced or reversed. This in turn would have reduced or eliminated the upwelling (contrary to a common assumption, upwelling is not solely a function of the wind stress but is coupled to the air–sea buoyancy flux too). The observed very close link between Antarctic temperatures and atmospheric CO_2 could then be explained as a natural consequence of the connection between the air–sea buoyancy flux and upwelling in the Southern Ocean, if slower ventilation of the Southern Ocean led to lower atmospheric CO_2. Here we use a box model, similar to those of previous authors, to show that weaker mixing and reduced upwelling in the Southern Ocean can explain the low glacial atmospheric CO_2 in such a formulation.

1. Introduction

The possibility that a change in the rate at which the deep sea is ventilated could lead to variations in atmospheric CO_2 was first raised in 1984, when several papers were published pointing to the possible role of the high-latitude oceans as controllers of natural CO_2 concentrations (Knox and McElroy, 1984; Sarmiento and Toggweiler, 1984; Siegenthaler and Wenk, 1984). The box models on which these 'Harvardton Bears' papers were based highlighted the dependence of atmospheric CO_2 on a balance between biological productivity and ventilation of the deep Southern Ocean. Today, water at the surface of the Southern Ocean contains non-zero mineral macronutrients (nitrate and phosphate) and, correspondingly, has a higher pCO_2 than would be the case if these nutrients were fully utilized. Much of the water in the deep sea is ventilated from this region, and its preformed nutrient and CO_2 concentrations are set at the surface of the Southern Ocean. Either increasing biological productivity, or decreasing the exchange of water between the surface and depth in this region, can cause atmospheric CO_2 to be lower in this kind of model.

The results of these papers were initially interpreted to suggest increased biological export production in the polar waters as an explanation of lower glacial CO_2. However, it has become increasingly clear that proxy evidence does not support the idea of an elevated Southern Ocean productivity in glacial time. There is room for doubt because not all proxies seem to tell the same story, but a recent 'multiproxy' compilation of last glacial maximum (LGM) export production estimates (Bopp et al., 2003) suggests a coherent picture: an increase in productivity in the sub-Antarctic region, particularly in the Atlantic sector, in glacial time, but less export production in the region South of (the present position of) the Polar Front.

An alternative possible explanation for lower glacial CO_2 is that the rate of ventilation of the deep ocean was slower in glacial time. Recently, Toggweiler (1999) has revived this idea as an

*Corresponding author.
e-mail: a.watson@uea.ac.uk
†Present address: National Oceanography Centre, Southampton, S014 3ZH, United Kingdom.
DOI: 10.1111/j.1600-0889.2005.00167.x

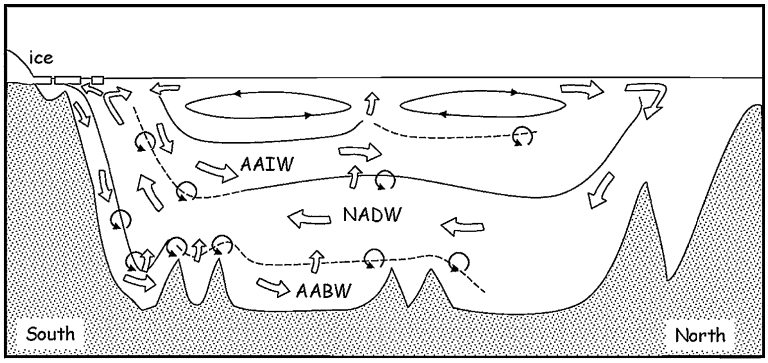

Fig 1. Schematic of the overturning circulation of the global ocean, represented as an average South-to-North section. See text for a description.

important mechanism for causing lower atmospheric CO_2. Given the substantial constraints put on the glacial CO_2 problem by the proxy evidence now available, a greater isolation of the deep ocean from the atmosphere seems necessary in any explanation. It is, however, not trivial to understand what may have caused this circulation change. In view of this, it is important to fully comprehend how 'southern component' deep water ventilates the ocean today. Accordingly, much of this paper is concerned with reviewing and clarifying this, using observations of the modern ocean. We then suggest why ventilation may have been different in glacial time. We make use of a box model to show that the mechanisms we propose, acting in combination with other effects that we know occurred, can change atmospheric CO_2 by the right amount in such box-type models. Ours is not the first suggestion of a mechanism to change ocean ventilation, and we therefore end by comparing our ideas with other recently proposed mechanisms, suggesting tests that may help to distinguish between the competing theories.

Our uncertainty about the causes of glacial-interglacial CO_2 change, even after more than 20 yr of research, is sometimes cited as an illustration of our ignorance of fundamental processes in the Earth system. However, though there are differences in the detail, it is worth noting that all the viable theories are now convergent in their most important aspects. Plausible explanations for lower glacial atmospheric CO_2 all share a requirement for increased isolation of the deep sea from the atmosphere ('slower ventilation'), obtained by one or more of the following: enhanced sea ice cover, increased near-surface stratification of the Southern Ocean, reduced upwelling or greater deep stratification in the same region. These changes serve to partition biologically fixed carbon into the deep sea and away from the atmosphere, lowering atmospheric CO_2. The higher carbon concentration at depth has a secondary but equally important consequence, in that it leads to an increased alkalinity of the ocean by 'carbonate compensation': deep water is acidified and becomes more corrosive to carbonate in sediments, so that ocean alkalinity increases until the source and sink of alkalinity are restored to balance. Both the increased efficiency of the carbon pumps and the increased alkalinity serve to lower atmospheric pCO_2 without requiring a large increase in biological productivity.

2. The global ocean overturning circulation

Figure 1 displays a schematic view of the global ocean overturning circulation, as represented by an average South-to-North section. The deepest, densest waters of the world ocean are formed close to the Antarctic continent, where saline, cold waters are produced by brine rejection associated with net sea ice formation at the continental shelf. These transfer into the deep ocean in down-slope gravity currents and by convection adjacent to the continent. In doing so, they mix with warmer and fresher circumpolar deep water to varying extents and result in distinct types of Antarctic bottom water (AABW) in each of the three major basins of the subpolar Southern Ocean (Orsi et al., 1999). As discussed further below, AABW is mixed up into lighter density classes while crossing the Southern Ocean; a fraction is thus returned towards the surface, while another escapes northward into the Atlantic, Pacific and Indian Ocean basins, forming the bottom waters there. North Atlantic deep water (NADW), less dense, warmer and more saline than AABW, is produced by convective sinking in the northern North Atlantic, and penetrates southward. Antarctic intermediate water (AAIW), freshened by net precipitation and sea ice melt, is formed by the convergence and mixing of Antarctic surface waters (transported northward by a net Ekman drift under the influence of the Southern Ocean westerly winds) with warmer upper-ocean waters to the north. AAIW penetrates northward to form the thermocline waters of much of the world ocean.

There are two contrasting views of the mechanics of the steady state overturning circulation. The classical view (Munk, 1966; Munk and Wunsch, 1998) is that the steady state circulation is governed by a balance between vertical advection and downward turbulent diffusion of buoyancy. In this 'abyssal recipes' picture, the rate-limiting step is how fast buoyancy can mix downwards. The vertical mixing rate, represented by the turbulent diapycnal diffusivity κ_z, is highly variable with position in the ocean. Measurements show κ_z to be very low in the thermocline (Ledwell et al., 1998) and the interior of the oceans away from rough topography (Toole et al., 1994). However, internal waves and turbulence generated by currents interacting with bottom topography induce enhanced mixing which can extend up

through the water column for several kilometres (Polzin et al., 1997; Ledwell et al., 2000). These mixing 'hot spots' are now thought to dominate the overall vertical mixing of the deep ocean.

The alternative view of the ocean overturning is that it is powered by wind-driven surface convergence and divergence, especially that associated with the westerlies in the Southern Ocean (Toggweiler and Samuels, 1995, 1998). In this view, the surface Ekman drift associated with the zonal winds near the latitude band of Drake Passage lifts water up from the deep ocean. This in turn allows a compensatory sinking of water elsewhere, that is, in the North Atlantic. This wind-driven overturning is not dependent on interior diapycnal mixing, and can proceed even as κ_z in the interior tends to zero.

Almost certainly, the real ocean is ventilated by a combination of both these modes. Given that rates of diapycnal mixing are agreed to be low in the main thermocline, advective processes, ultimately wind driven, likely dominate vertical transport through the top kilometre or so of the water column over most of the world ocean. A fraction of the NADW formation is probably wind driven by Ekman suction in the Southern Ocean, see for instance Webb and Suginohara (2001). On the other hand, the ventilation of the densest waters in the world ocean must be largely diapycnally driven. This seems inevitable, because this water has no surface outcrop of significant area—it is formed in a few special places, in dense but areally restricted plumes associated with shelf processes or convection. There is no known mechanism to return it to the surface so as to be destroyed by air–sea interaction in these same highly confined regions, so its return must involve modification to less dense water in the interior. On tracing the path of this water away from the Antarctic, it becomes clear (see e.g. Mantyla and Reid, 1983) that it is modified in this way, its properties being altered in the deep sea, well away from the surface, implying large interior diapycnal transformations. Therefore, if ventilation of the deepest ocean was slower in glacial than interglacial time, as Toggweiler (1999) suggested, this is likely to be at least partly a question of changing diapycnal mixing rates. This presents a theoretical challenge. Why should deep ocean mixing be weaker in glacial time? In fact, there is at least one line of reasoning to suggest that turbulent mixing should have been *stronger* in the deep glacial ocean: tides, which provide a primary energy source for deep ocean mixing, must have been more vigorous in the glacial ocean because of the lower sea level (Egbert et al., 2004).

Recently, Munk and Wunsch (1998) have pointed out that the energy required to drive the abyssal circulation is of the same order as the total energy available from wind- and tidally generated currents in the deep sea. Plausibly, therefore, the overall control on the rate at which the deep overturning circulation turns is one of energy limitation. The power required to sustain the diabatic abyssal circulation is readily calculated. From a scale analysis, the rate at which potential energy must be added to raise bottom water being formed with a volume flux of Q is $W \sim Q\Delta\rho gh$, where $\Delta\rho$ is the difference between the initial and final densities of the water, g the acceleration due to gravity and h is the scale height of the density change. If the available power supply is constant, then, other things being equal, Q might be expected to be inversely related to $\Delta\rho$, with the total buoyancy flux $Q\Delta\rho$ remaining constant. Similarly, scale analysis of the steady-state advective–diffusive balance (e.g. that employed by Munk, 1966) gives us the relation $Q \sim A\kappa_z/h$ between the overturning rate, the area A over which upwelling occurs, the vertical mixing rate and the scale height. Substituting for Q in the first expression we obtain $W \sim A\kappa_z\Delta\rho g$, demonstrating that if the power is indeed constant then vertical mixing rates should be inversely proportional to density difference. Recent articles by Nilsson and colleagues (Nilsson et al., 2003, 2004) have explored in greater detail the implications of an energy-limited overturning for the modern day circulation with conceptual and numerical models. Here we simply note that there are reasons to believe that mixing and overturning rates may decrease as density anomaly increases. Suppose then that in glacial time the density contrast between the deepest waters and those overlying them was greater than it is today; this might help explain why the deep sea was apparently less well ventilated at the LGM.

What do we know about the stratification of the deep ocean in glacial time? Figure 2, redrawn from Adkins et al. (2002), shows estimates of the temperature and salinity in the deep ocean at the LGM reconstructed from measurements on pore waters, compared with present-day conditions. Contours of potential density anomaly referenced to 4000 decibars (σ_4) are also shown. The difference between the stratification of the glacial and modern ocean is striking. Salinities are greater everywhere, which is to be expected because the greater volume of freshwater bound up in icecaps in glacial time resulted in a more saline ocean. However, whereas the modern abyssal ocean is largely stratified by temperature differences, the density differences in the deep glacial ocean are mostly due to salinity. Temperatures are close to freezing at all the sites in the glacial ocean, but the deep Southern Ocean site (which lies within a primary AABW spreading pathway in the modern ocean) reveals itself as much more saline than the other locations. The density anomaly between the Southern Ocean site and the others is about three times larger than it is today, and a crude application of the above (much over-simplified) reasoning might then suggest that the mixing between this southern component and the overlying waters was three times slower at the LGM. Salinity conservation suggests that, if the calculation of the mean salinity of the glacial ocean is correct, a substantial volume of the intermediate and upper ocean waters (for example, glacial AAIW) must have been considerably fresher than the deep waters.

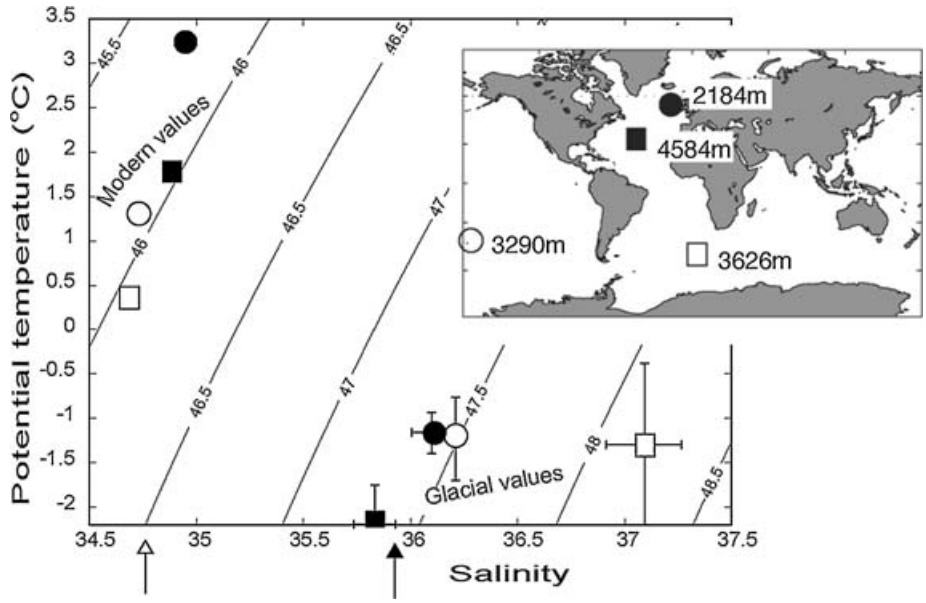

Fig 2. Potential temperature-salinity diagram of deep waters at the LGM derived from pore water measurements at four Ocean Drilling Project sites by Adkins et al. (2002). The modern values at these sites are also shown. Contours are of σ_4. The open arrow shows the modern mean ocean salinity, while the filled arrow is the average salinity adjusted for a 125 m drop in eustatic sea level, similar to that at the LGM. The inset shows the locations of the four sets of measurements, with the depths in metres written by each symbol. (Redrawn from Adkins et al., 2002.)

3. Mixing and ventilation of the modern-day Southern Ocean

3.1. Diapycnal mixing in the deep

In recent years a good deal of new information has become available relating to rates of diapycnal mixing in the Southern Ocean. In the near surface there have been several direct measurements using tracer releases (Law et al., 2003; Goldson, 2004). In the region of the Scotia Sea, studies making use of new techniques applied to lowered acoustic Doppler current profiler (LADCP) velocity measurements have suggested widespread high mixing rates at a large range of depths (Naveira Garabato et al., 2004; Heywood et al., 2002). Estimates using chlorofluorocarbons (CFCs) in the broad plume of bottom water originating from the Weddell Sea and flowing toward the Indian Ocean have also indicated high rates of mixing between this and the overlying water (Haine et al., 1998). These estimates are drawn together in Table 1. There is a considerable range of values, particularly in the deep ocean, reflecting the dominant influence of topography. However, a consistent picture emerges: in the upper water column, mixing across and below the summertime seasonal pycnocline is $\sim 10^{-5}$ m^2 s^{-1} (although rates may be several times higher during the passage of storms (Goldson, 2004). In the

Table 1. Estimates of diapycnal mixing rates in the Southern Ocean

Source	Method	Depth	Location	Value (10^{-4} m^2 s^{-1})
Upper water column				
Law et al. (2003)	SF_6 tracer release	50–100 m	61°S, 140°E	0.11 ± 0.2
Naveira Garabato et al. (2004)	LADCP shear and internal wave-wave interaction model	50–300 m	SE Pacific, SW Atlantic	0.1–0.3
Deep water				
Haine et al. (1998)	CFC budget	>3500 m	Abyssal S. Ocean 20°W–60°E	5 ± 2
Heywood et al. (2002)	LADCP-referenced transport and basin budget	>3500 m	Scotia Sea	39 ± 10
Naveira Garabato et al. (2004)	LADCP shear and internal wave–wave model	>2000 m	Scotia Sea Western Drake Passage	5–100 10–1000
This study	CFC and mass budgets	>2000 m	Atlantic, Pacific and Indian basins	~10

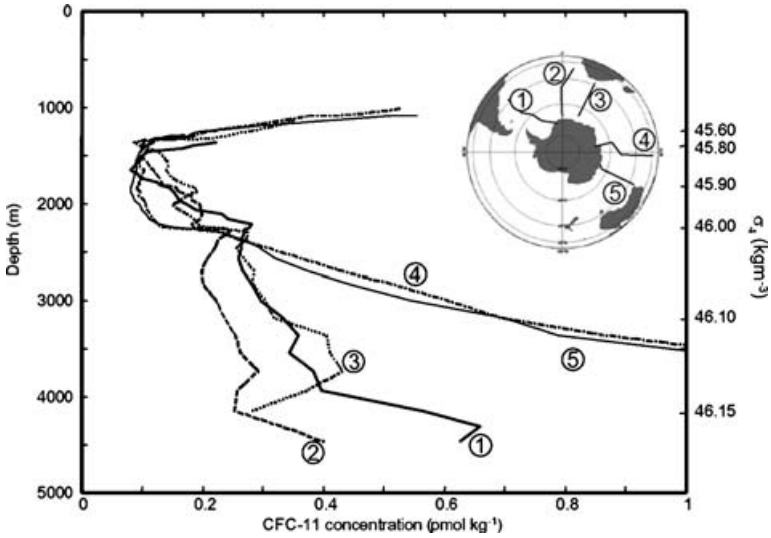

Fig 3. Average CFC-11 profiles for WOCE sections in the Atlantic and Indian sectors of the Southern Ocean. The profiles are averaged along σ_4 surfaces, south of 50°S. They are displayed against depth using a density-to-depth mapping which is the mean depth of the isopycnals from the same data set.

Atlantic sector of the deep Southern Ocean, however, rates are $\sim 10^{-3}$ m^2 s^{-1} below 3500 m, attaining even higher values immediately above rough topography. Results of inverse models constrained with hydrographic data also suggest vigorous diapycnal transformations in the deep Southern Ocean (Ganachaud and Wunsch, 2000; Sloyan and Rintoul, 2001), but the uncertainties in those estimates are large.

As shown, for example, by Haine et al. (1998), CFC concentrations can be useful for illuminating the processes of ventilation from the surface to the interior of the Southern Ocean. Figure 3 shows the mean CFC concentration profiles for the Atlantic and Indian World Ocean Circulation Experiment (WOCE) sections, averaged over regions South of 50°S. Concentrations were averaged along surfaces of constant σ_4 and are plotted as a function of depth after transforming into depth coordinates, using the average depth versus σ_4 relationship. CFCs are readily detectable throughout the water column. CFC sourced at the bottom from outflowing AABW mixes up through the water column to depths of ~2000 m, especially due to the very intense mixing in the Scotia Sea. If we assume that the bottom is the origin of the mid-depth CFC signal, a simple scale analysis can be used to estimate the order of magnitude of the vertical mixing rate that must be responsible: CFCs have a time scale for increase in the atmosphere on the order of 20 yr. The deep profiles in Fig. 3 have length scales on the order of 1000 m or more. From these scales, a mixing rate $\kappa_z \sim$ (length scale)^2/(time scale) $\sim 10^{-3}$ m^2 s^{-1} follows, for the Atlantic and eastern Indian sectors. This is compatible with the deep mixing rates obtained by other authors, as summarized in Table 1. It is about 10 times the canonical average calculated for the world ocean below ~1000 m by Munk (1966).

It is probable that not all the mid-water CFC content in Fig. 3 comes from up-mixing from the bottom source. Some shelf water of less extreme density likely ventilates the circumpolar deep water at the Weddell–Scotia confluence (Whitworth et al., 1994) and contributes to the mid-depth CFC concentrations. For this reason, the above order-of-magnitude calculation of diapycnal mixing may produce an overestimate when applied away from the bottom 1000–2000 m.

We now make a more detailed estimate of the rates of mixing in the deep Southern Ocean, exploiting the fact that the densest isopycnal surfaces ($\sigma_4 > 46.1$ kg m^{-3}) are confined to the basins there, so that the net production of bottom water with density in excess of any such σ_4 value can be equated to the upwelling through the relevant isopycnal. We start from the equation for the flux F of potential density σ across an isopycnal surface:

$$F = \sigma w - \kappa_z(\partial\sigma/\partial z),$$

where we have used z, w and κ_z to signify distance, velocity and eddy diffusivity normal to the surface, which in practice will be very close to vertical. We evaluate the flux over a surface A of constant potential density σ_A in the deep Southern Ocean. The isopycnal surface is bounded by its intersection with the ocean floor, except where it abuts the formation regions of bottom water. Integration of the flux over the surface gives:

$$\iint F \, \mathrm{d}A = \iint \{w\sigma_A - \kappa_z(\partial\sigma/\partial z)_A\} \, \mathrm{d}A.$$

In a steady state, this integral is equal to the rate of injection of mass by bottom water formation, $V\sigma_i$, where V is the volume rate of formation and σ_i the potential density at formation. Equating the volume of water being injected to that flowing through the surface, that is, $\iint w \, \mathrm{d}A = V$, we obtain:

$$\begin{aligned} V(\sigma_i - \sigma_A) &= -\iint \kappa_z \, (\partial\sigma/\partial z)_A \, \mathrm{d}A \\ &= -\overline{\kappa_z} \iint (\partial\sigma/\partial z)_A \, \mathrm{d}A \end{aligned} \quad (1)$$

where we have defined $\overline{\kappa_z}$ as the mean diffusivity weighted by the potential density gradient over the surface. The integral on

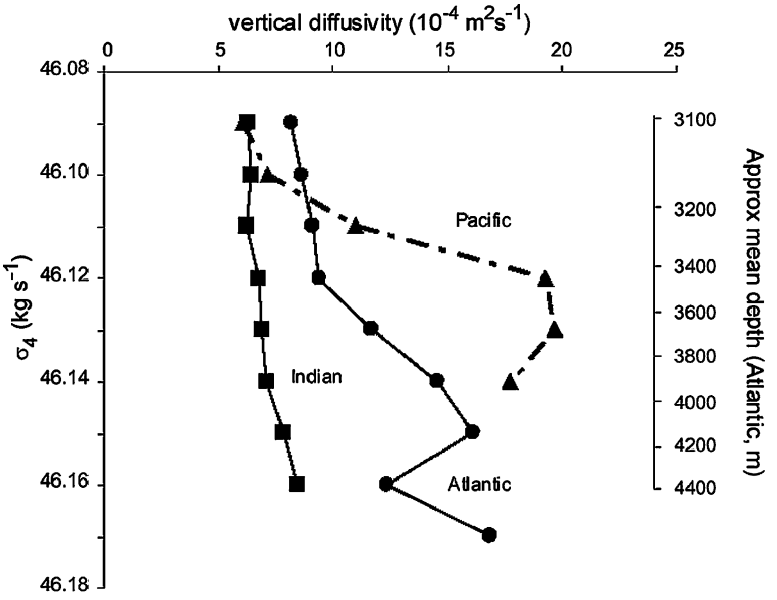

Fig 4. Average diapycnal mixing coefficients in the three abyssal basins of the Southern Ocean, calculated from World Ocean Atlas 1998 1°-gridded annual mean densities and bottom water formation rates derived by Orsi et al. (1999), by the method described in the text. The analysis is conducted in density space. The scale on the right gives approximate depths based on the density-depth relationship in the Atlantic basin.

the right-hand side can be evaluated using climatological hydrographic data.

Estimates of the volume rate of formation and potential density at formation for four types of bottom water may be obtained from the work of Orsi et al. (1999). The method employed by these authors was based on a detailed inventory of CFCs, from which they deduced an overall production rate of AABW of 8.1–9.4 Sv (1 Sv = 10^6 m^3 s^{-1}), defined as the rate at which new bottom water crosses the 2500 m isobath moving away from the continent. Approximately 60% of this goes into the Atlantic basin and 40% into the combined Indian and Pacific basins. Using the data from their Table 4 to evaluate the left-hand side of eq. (1) and the World Ocean Atlas 1998 (http://www.nodc.noaa.gov/OC5/data_woa.html) to evaluate the integral on the right-hand side, we estimate $\overline{\kappa_z}$ averaged over the Atlantic, Indian and Pacific sectors, as a function of σ_4 or σ_2, with results shown in Fig. 4. We exclude regions shallower than 2500 m from the calculation, since these are also excluded in Orsi et al.'s analysis as being the formation regions of the bottom water. For the Atlantic Weddell–Enderby basin the volume rate of formation and its source are unambiguous. For the other two basins (the Australian Antarctic and Pacific Antarctic) the partitioning of bottom water formation rates is not defined by Orsi et al. We choose to partition the formation rates as 60% to the Australian Antarctic basin and 40% to the Pacific Antarctic basin, based on the inference by Rintoul (1998) that up to 25% of the circumpolar AABW production occurs in the Indian Ocean.

The analysis confirms, basin-wide, that mixing rates are high in the deep Southern Ocean, of order 10^{-3} m^2 s^{-1}, and that they increase with depth. Values are well above the 'abyssal recipes' average for the world ocean below ~1000 m of 10^{-4} m^2 s^{-1}. Since the Southern Ocean encompasses about 10% of the global ocean, the calculation suggests that this region alone is responsible for a disproportionately high fraction of the global deep mixing. The effect of this rapid mixing on the properties of newly formed AABW is substantial, with the bottom waters becoming considerably less dense to the North of the ACC. Thus, in the process of transiting away from its formation regions, AABW upwells into the lighter density classes. For example, according to the measurements of Haine et al. (1998), the Weddell Sea AABW has a transit time to the Crozet-Kerguelen region of only ~40 yr, but this is long enough for its potential temperature to rise from less than −0.4°C to about 0.5°C. Thus, the AABW that fills the abyss of most of the world's oceans is substantially less dense than the water that first sinks to great depth in the Southern Ocean.

It seems clear that the chief energy source for this rapid mixing must be the interaction of deep geostrophic boundary currents (including those associated with the ACC) with the bottom topography. Southern Ocean mixing is thus primarily wind driven, while the turbulent diapycnal mixing in the deep ocean basins further north is likely powered by tides to a larger extent and associated with mid-ocean ridge processes (Munk and Wunsch, 1998). Modelling studies (Egbert et al., 2004) suggest that tidally driven mixing in the deep ocean may have been more intense in glacial time than at present, possibly raising the globally integrated diapycnal mixing rate at the LGM. In spite of this, the weakening of diapycnal mixing in the deep glacial Southern Ocean must have led to a net lengthening of the pathway by which dense water sinking in the Southern Ocean upwells into lighter density classes and is ultimately returned to the upper ocean. In following that pathway, the dense Southern Ocean water would have had to transit to the mixing centres in the distant ocean basins to the North rather than be 'short-circuited' in the Southern Ocean.

We conclude that diapycnal mixing serves to transport bottom waters rather rapidly up to a depth of ∼2000 m in the Southern Ocean. Closer to the surface, observations suggest that diapycnal mixing falls to values of $\sim 10^{-5}$ m^2 s^{-1}. However, in this depth range there is a vertical circulation that can act to lift the water towards the surface, completing a pathway of relatively rapid ventilation of the deep water. We now summarize briefly current ideas about this circulation.

3.2. *The meridional overturning circulation in the modern ACC*

The mid-depth waters of the Southern Ocean participate in a meridional overturning, made up of a wind-driven Ekman circulation and an opposing flow associated with mesoscale eddies (e.g. Speer et al., 2000; Karsten and Marshall, 2002; Bryden and Cunningham, 2003). Building on earlier studies (Walin, 1982; Marshall, 1997), Karsten and Marshall (2002) recently analysed the residual mean circulation—the net meridional overturning averaged in time and around the path of the ACC—using a combination of observations and theory. Here we summarize their conclusions as they are relevant to our discussion.

It is convenient to define a streamfunction $\Psi_{\rm res}(y, z)$ for the residual mean overturning, such that the northward and upward residual mean velocities are given by

$$v_{\rm res} = -\partial\psi_{\rm res}/\partial z, w_{\rm res} = \partial\psi_{\rm res}/\partial y.$$

One component of the streamfunction, contributing a northward velocity at the surface, is the wind-driven Ekman transport. This is directly related to the westerly wind stress, averaged in time and integrated around the path of the ACC. A second component, acting in the opposite direction near the surface, relates to the net eddy transport resulting from baroclinic instability in the ACC. $\Psi_{\rm res}$ is the sum of the two. Karsten and Marshall showed that the following relation must also apply to $\Psi_{\rm res}$ at the base of the mixed layer with depth h_m:

$$\psi_{\rm res}(z = -h_m)\partial b_m/\partial y = B - \kappa_z \partial b/\partial z(z = -h_m), \qquad (2)$$

where b represents buoyancy (defined as $-g\sigma/\rho_0$, with ρ_0 as a reference density), b_m is the buoyancy of the mixed layer, and B is the buoyancy flux entering or leaving the ocean surface. The last term, $-\kappa_z\, \partial b/\partial z(z = -h_m)$, is the vertical flux of buoyancy across the mixed layer base. If κ_z is small (as the near-surface measurements in Table 1 suggest) then this term can be neglected.

Equation (2) expresses the balance between the air–sea heat and freshwater fluxes and the net overturning circulation. The left-hand side is the streamfunction times the meridional gradient of buoyancy in the mixed layer. $\partial b_m/\partial y$ is positive, meaning that as one travels northward the surface water becomes lighter. If the residual stream function is also positive (implying a net northward transport of surface water) the water must become less dense as it moves. Buoyancy must therefore be added to it. The required buoyancy flux is given by the right-hand side of the equation and is dominated by the air–sea flux B. Estimates of the magnitude of the upwelling South of the Polar Front vary, but Karsten and Marshall suggest that the Ekman flux is about 21 Sv and the eddy flux is about 8 Sv, leaving a net northward/upward flux of 13 Sv.

How, in practice, does the ocean achieve the balance expressed by eq. (2)? Does the residual circulation adjust to match the buoyancy flux from the atmosphere, or vice versa? Today, the air–sea heat transfer appears to dominate the net buoyancy gain by the ocean in the ACC (see e.g. Karsten and Marshall, 2002), but the net heat flux involved is not large (∼10 W m^{-2}). If the net northward transport of water were to increase, this would entail more cold water moving north, leading naturally to a greater air–sea heat transfer that would tend to restore the balance. Thus, today, the net buoyancy flux into the ACC probably responds to the residual circulation, rather than vice versa.

However, when we try to imagine how the system behaves in glacial time, it will be of interest to follow what would happen if the buoyancy flux did not increase in this way with a stronger northward drift, as might be the case if it is dominated by the freshwater flux. In that case, increasing the wind stress would lead to a stronger northward Ekman flux, which would upwell subsurface water to the South and increase the North–South tilt of the isopycnals. This increased baroclinicity would result in a larger eddy flux that would oppose the Ekman flux. If the net air–sea buoyancy flux were constant then, from eq. (2), the steady-state residual circulation would tend to remain unchanged, so the increase in the eddy flux would continue until the increase in the Ekman flux was largely balanced.

3.3. *The meridional overturning circulation in the glacial ACC*

Proxy evidence suggests that at the LGM, the area covered by sea ice in winter in the Southern Ocean was about twice the ∼1.8 × 10^{13} m^2 that is covered today, and extended more or less to the present position of the Polar Front (Gersonde and Zielinksi, 2000; Crosta et al., 1998a,b). In winter, therefore, water arriving at the surface tended to freeze, implying a net buoyancy flux out of the ocean. Proxies for the position of the ice edge in summertime are more equivocal: Gersonde and Zielinksi argue that at the LGM the summer ice edge was near the present-day winter ice maximum, while Crosta et al. suggest it was not very different from the modern summertime ice extent.

Today, seasonal sea ice does not encroach into the region where the main transport of the ACC occurs (the wintertime ice limit lies mostly near 60°N, although it extends further north in the Atlantic sector where the ACC also shifts northward). The permanently open water on the southern flank of the ACC can readily take up heat from the atmosphere as well as freshwater from net precipitation and ice melt, and the circumpolar eastward flow can be sustained with a relatively large residual circulation and associated upwelling of deep water. In glacial time, the ACC

may have been broadly at the same latitude (as suggested by its profound dynamical link with topography—see Olbers et al. (2004) for a review) and its poleward flank was likely subject to seasonal ice cover, implying little buoyancy gain due to air–sea heat exchanges. Although there may have been buoyancy gain due to net ice melt in part of this region, analogy with the modern subpolar seas suggests that this would have been smaller than the predominantly heat-driven buoyancy gain in the modern ACC. If the surface buoyancy gradient across the glacial ACC was similar to that in the modern ocean (as may be expected from the cross-ACC density contrast being largely set by the magnitude of the wind stress, Gent et al., 2001), the implication is that the upwelling supported by the air–sea buoyancy flux would have been correspondingly less. The vigorous upwelling that today occurs south of the Polar Front would not have been present.

Invoking mass conservation, any buoyancy gain in the ACC due to net ice melt must be accompanied by buoyancy loss due to net ice formation further south. However, buoyancy loss associated with net ice formation is only efficiently exported from the surface where it occurs over the continental shelf and can drain into the deep ocean. This suggests that, in glacial time, there may have been a stronger connection between bottom water formation and upwelling in the ACC than exists today, by virtue of the buoyancy and stratification being largely salinity driven rather than temperature driven: the extent to which deep water was upwelled in the ACC by the residual circulation would thus have been limited by the formation rate and density of AABW.

A change in the mean upwelling in the Southern Ocean would be likely to have consequences for the global overturning circulation. The 'Toggweiler and Samuels' view (Toggweiler and Samuels, 1995, 1998) is that the formation of NADW in the North Atlantic is governed by upwelling in the Southern Ocean, which we have argued above is linked to, and to some extent controlled by, Southern Ocean net air–sea heat and freshwater fluxes. Some of the consequences of this linkage have been explored by Keeling (2002) and Keeling and Stephens (2001) who focus on the role of freshwater forcing at high southern latitudes and argue that aspects of climate instability associated with the 'conveyor belt' circulation can be accounted for by this model. Here we do not attempt to explore this complex subject in detail, but we do note that the probable reduction in NADW formation in glacial time would be consistent with decreased upwelling in the Southern Ocean, and the two may be causally linked.

3.4. Summary of changes in ventilation between the LGM and present

The proxy evidence suggests that in glacial time there was a larger coverage of Antarctic sea ice, extending in winter up to the present position of the Polar Front but melting back in summer. There is evidence too that bottom waters were considerably more saline than they are today and that the deep ocean was more stratified, with the stratification being due to salinity rather than temperature and bottom temperatures being close to freezing through much of the world ocean. Presumably the very cold and saline bottom water was formed by a more extreme production of brines over the Antarctic shelf due to net sea ice formation. The greater stratification led to slower mixing in the deep water, reducing the up-mixing of the deepest waters into the overlying layers. The colder atmospheric temperatures and seasonal sea ice coverage reduced net air–sea heat fluxes, leading to less upwelling South of the Polar Front and tending to further isolate the deepest waters from the surface. At the same time, formation of warm and saline NADW was reduced substantially. The result was an ocean in which high salinity was mostly partitioned towards the coldest waters. In this ocean, the main density division was between the fresh AAIWs and the saline bottom waters, which filled the major ocean basins.

4. Effect of circulation changes on atmospheric CO_2

4.1. Build up of inorganic carbon in deep waters

Isolating the deepest water in the world's ocean from the atmosphere may be expected to alter the natural concentration of atmospheric carbon dioxide for a number of linked reasons. In particular, the 'biological pump' tends to partition carbon towards the deep sea, the carbon being re-equilibrated with the atmosphere when the water is returned to the surface. Increasing the residence time of the water in the deep ocean, therefore, allows more time for biologically transported material to build up in the bottom waters, thereby removing it from the surface water and contact with the atmosphere. Furthermore, increasing the total carbon content of the deep water by remineralisation of organic material lowers its pH, causing the lysocline to become shallower, and some carbonate in deep sea sediments or in particles falling to the ocean floor to dissolve more readily. This increases the alkalinity of the ocean, which further reduces the pCO_2 of surface waters. Given a step change in the deep ocean pH, due for example to a change in deep sea ventilation, this 'carbonate compensation' might be expected to continue until the rate of output of alkalinity to sediments matches the rate of input to the oceans as a whole—which is due to weathering products coming from the land via rivers, and to a first approximation might be considered constant. This implies that the lysocline will, on a time scale set by the sedimentary interaction, return to roughly the same depth that it was previously at, but now with a higher mean alkalinity. There is good evidence that the mean position of the lysocline did not change much between the LGM and the present day, though it shallowed somewhat in the Atlantic and deepened a little in the Pacific (Anderson and Archer, 2002). We know of no other source than the ocean for the CO_2 that has increased in the atmosphere (and also in the terrestrial biosphere) since glacial time. If this carbon had been removed from the

ocean without any change in alkalinity, it would have caused the lysocline to deepen. The fact that today the lysocline seems to be in the same position as it was at the LGM, therefore, suggests that carbonate compensation has gone essentially to completion since the LGM.

4.2. Modelling the effects of circulation change

Box models of the ocean–atmosphere carbon system were used by the Harvardton Bears papers, and continue to be used to explain glacial-to-interglacial atmospheric CO_2 change (Toggweiler, 1999; Stephens and Keeling, 2000). Three-dimensional ocean carbon general circulation models (OCGCMs) have also been applied to this problem since the late 1990s (Broecker et al., 1999; Archer et al., 2000a; Bopp et al., 2003; Toggweiler et al., 2003a). It has been found that box models usually display substantially higher sensitivity to high-latitude processes than do the OCGCMs (Broecker et al., 1999). The high-latitude mechanisms put forward, for example by Toggweiler (1999), Watson et al. (2000) and Stephens and Keeling (2000), are relatively ineffective when simulated in such ocean carbon models. The reasons for this different behaviour have been investigated by Archer et al. (2000b) and Toggweiler et al. (2003a,b). There is not as yet a general agreement on the causes, however. For example, Archer et al. experimented with several different OCGCMs, finding that when a level model was modified to rotate the mixing tensor into alignment with isopycnal surfaces (Redi, 1982), thus removing one (but not the only) source of unphysical diapycnal mixing, this resulted in a more acute high-latitude sensitivity. However, an isopycnic co-ordinate model, which should have little unwanted cross-isopycnal diffusion, showed relatively weak high-latitude dependence, so these authors were unable to unambiguously ascribe the low sensitivity of OCGCMs to diapycnal diffusion alone.

It is clear that altering diapycnal mixing in a model may substantially affect the CO_2 concentration of its atmosphere. This is important because, as discussed above, the distribution of diapycnal mixing in the real ocean is poorly known. Existing OCGCMs almost certainly do not reproduce it well and, furthermore, numerical diffusion effects may mean that the true diapycnal leakage in many ocean carbon models is not well understood. If diapycnal diffusion is zero, the potential density of a water parcel is fixed once it has left the surface (because conserved properties are invariant in a Lagrangian frame of reference when diffusion is zero, see for example, Gill (1982), while isopycnal diffusion cannot, by definition, transport density). In such an ocean, water parcels must then return to the surface with the same density as they left it. Since most deep ocean isopycnals outcrop only in the high-latitude areas, the interaction of the bulk of the ocean with the atmosphere will then be governed largely by conditions in those outcropping regions. However, in the presence of diapycnal mixing, water parcels return to the surface with a lighter density and a higher temperature than they left it, tending therefore to outgas CO_2 on reaching the surface. Thus, increasing the diapycnal mixing in a model will tend to raise the predicted atmospheric CO_2 concentration, and make it more difficult to partition the CO_2 into the deep sea and away from the surface. These considerations suggest (in accord with Archer et al.'s results using level models) that a reduction of diapycnal mixing should cause a model to have a greater sensitivity to high-latitude processes. Since in box models the diapycnal mixing can be specified to be arbitrarily low, whereas in coarse-resolution OCGCMs the effective diffusivity may be raised by numerical effects and be poorly characterized, it is at least possible that the real ocean behaves more like a box model than such an OCGCM in this particular regard.

Toggweiler et al. ascribe the difference in behaviour of OCGCMs and box models to the smaller outcrop areas of polar waters in the former, and to unrealistic treatment of ice cover of these outcrops. In the current generation of OCGCMs being used to address this problem, production of bottom water is normally parameterized by deep convection, occurring in the open ocean at the grid scale (i.e. typically a degree or more in linear dimension). In the real Southern Ocean, however, bottom water formation is intimately associated with shelf and ice formation processes. Convection is localized to much smaller scales and reaches the bottom only over the continental shelf. Toggweiler et al.'s work suggests that, for the CO_2 problem, the source of the densified water formed over the shelf and the degree of mixing with ambient waters during transfer to the deep sea are critical in determining the natural concentration of atmospheric CO_2 at steady state with the ocean. Because such processes are not accurately parameterized in current OCGCMs, and are arbitrarily specified in box models, neither representation can be physically justified.

Thus, despite the obvious superiority of GCMs over box models when reproducing wind-driven horizontal circulations, it is by no means certain that this superiority carries over to simulations by OCGCMs of the effect of circulation or biology changes on atmospheric CO_2. In the following we describe the use of a simple box model to demonstrate that, at least in that context, the mechanisms we have described have a substantial effect on atmospheric CO_2. We use a box model because it is more transparent and easier to understand in comparison to readily available OCGCM-based carbon models, but we caution that existing OCGCMs would not show as much sensitivity to the Southern Ocean processes. Nevertheless the box model is not set up to be deliberately sensitive to high-latitude regions (the overall vertical exchange rate is not artificially low, for instance).

The model is similar in general type to that used by Toggweiler (1999) to show that changing ventilation rates in the deep sea does affect atmospheric CO_2. Stephens and Keeling (2000) employed a similar model to investigate the effect of blocking gas exchange by dense ice cover in the Southern Ocean. The model is shown in Figs 5a–d, where the circulation and steady state modern and glacial solutions are displayed,

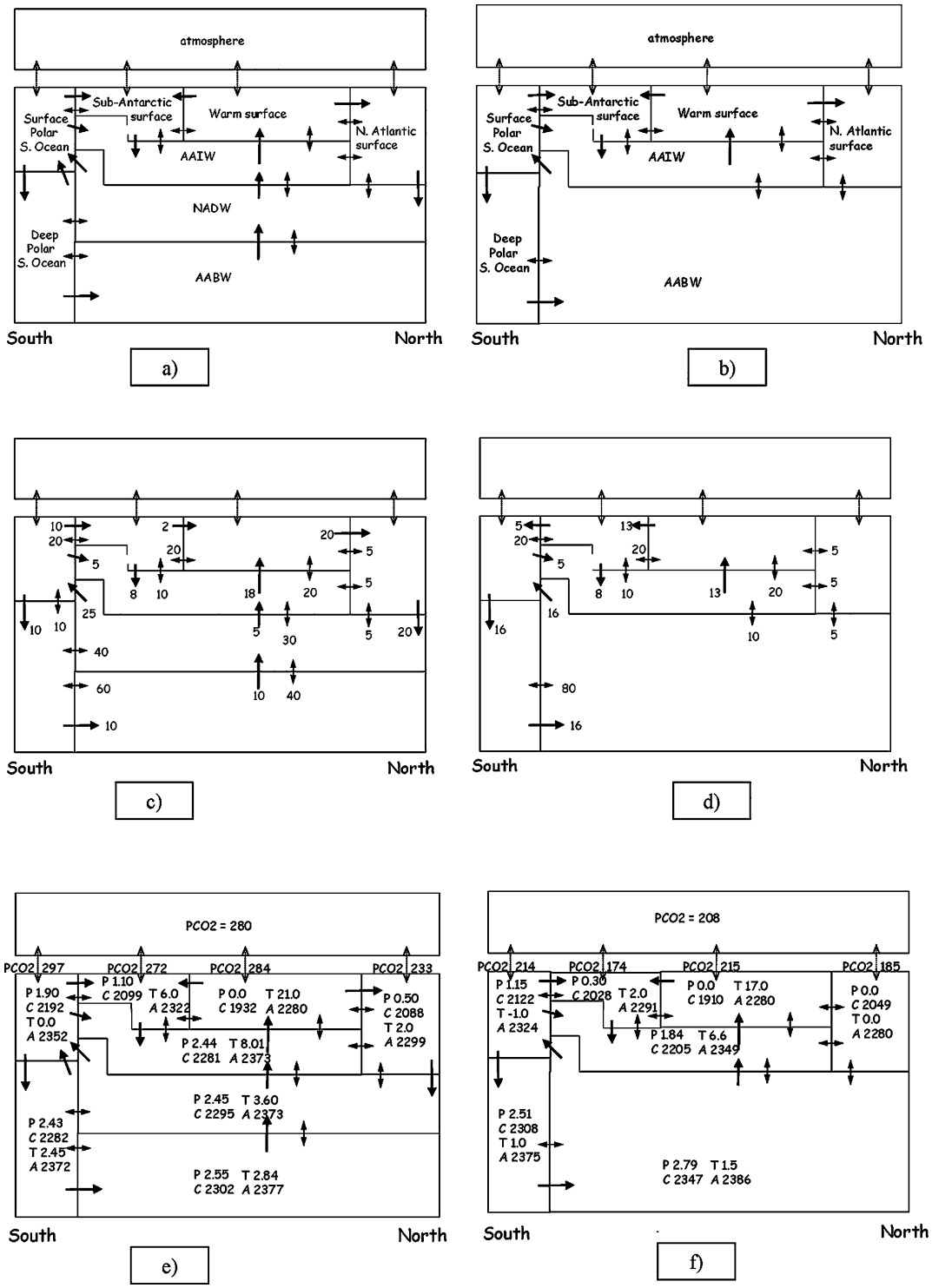

Fig 5. The reservoir-flux model of the ocean and atmosphere used to investigate the influence of changing vertical circulation on atmospheric CO_2. Figures 5a and 5b label the boxes in the model for the 'modern' and 'LGM' circulations—see Table 2 for further details on the reservoir sizes. Figures 5c and 5d show the magnitudes in Sv (1 Sv = 10^6 m^3 s^{-1}) of the flows connecting each box for the two circulations, where a single-headed arrow indicates a flow in one direction, and a double-headed arrow indicates an exchange flux. Figures 5e and f show the values for the four variables in the modern and a LGM run (C = total carbon, P = phosphate, A = total alkalinity, all in μmol kg^{-1}, and T = temperature in °C). The LGM configuration shown is that of column 5 in Table 3, before carbonate compensation is applied. Thus the inventories of phosphate, alkalinity and carbon are the same in Figs 5e and 5f.

Table 2. Parameters of the box model (see also Fig. 5)

Volume of global ocean 1.35×10^{18} m^3		Area of global ocean 3.5×10^{14} m^2		Volume of the atmosphere 1.66×10^{20} moles	
		Surface reservoirs			
		Southern Ocean surface	sub-Antarctic surface	Warm surface	North Atlantic surface
	Fractional area	0.07	0.08	0.8	0.05
	Fractional volume	0.02	0.03	0.07	0.02
		Subsurface reservoirs			
		Fraction of export production from surface boxes remineralised in each sub-surface box			
	Fractional volume				
Antarctic intermediate	0.2		0.4	0.4	0.4
North Atlantic deep	0.29	0.1	0.4	0.4	0.4
Deep Polar Southern	0.1	0.9			
Antarctic Bottom Water	0.27		0.2	0.2	0.2

together with other details in Table 2. The model has some variations from those of earlier authors to allow investigation of the particular processes we have been discussing. It has eight boxes to represent the global ocean, based on the major water mass types. The surface ocean is divided into Polar Antarctic, sub-Antarctic, northern North Atlantic and the rest (the 'warm surface ocean'). The subsurface ocean is divided into AAIW, NADW and AABW. A separate reservoir is included to represent the coldest AABW in the deep Southern Ocean.

Figures 5a and 5c show 'modern' and 'LGM' circulations as represented in the model. In the modern case, the Atlantic meridional overturning circulation is represented by a 20 Sv formation of NADW, of which 5 Sv upwells into the AAIW reservoir while the rest upwells in the Southern Ocean (Webb and Suginohara, 2001). A total of 20 Sv of southern component bottom water is formed (see e.g. Sloyan and Rintoul, 2001), of which half is quickly returned to the surface by the mixing processes discussed above, while the rest goes on to form the AABW found in the bottom of the major ocean basins. The deep Southern Ocean is mixed with NADW, so that the bottom water of the Southern Ocean is warmed and modified before spreading to the rest of the world ocean. A total of 13 Sv of AAIW is formed at the equatorward flank of the ACC (see e.g. Talley, 1999), of which 8 Sv is drawn from the Sub-Antarctic surface and 5 Sv from the Polar Southern Ocean. The net advective input to the AAIW reservoir is thus 18 Sv (including 5 Sv produced by upwelling of NADW) and this is assumed to upwell into the warm surface reservoir.

Vertical mixing between reservoirs is represented by exchange fluxes of water. In the main ocean basins, these approximately mimic what we know about vertical mixing there. For reservoirs 1000 m deep covering the temperate and tropical oceans (an area of $\sim 3 \times 10^{14}$ m^2 s^{-1}) a vertical diffusivity of 10^{-4} m^2 s^{-1} corresponds to an exchange flux of $\sim 10^{-4} \times 3 \times 10^{14}$/ 1000 m^3 s^{-1} = 30 Sv. Rates of 40, 30, and 20 Sv were typically used for the exchange between, repectively, AABW–NADW, NADW–AAIW, and AAIW–surface, corresponding to vertical mixing that increases with depth. The relatively high value for the main thermocline is meant to reflect not only diapycnal exchange there (which alone, given diffusivities of $\sim 10^{-5}$ m^2 s^{-1}, would suggest a value <5 Sv) but also ventilation of the thermocline by wind-driven and eddy effects.

In the LGM circulation, NADW formation is turned off and the AABW and NADW reservoirs combined to give a single large AABW reservoir. Increased density contrast is assumed to slow the exchange between this water and the AAIW above it, and following our earlier discussion we set a value, which is one third of that at the same boundary in the modern circulation (10 Sv, corresponding to a diapycnal mixing rate of $\sim 3.3 \times 10^{-5}$ m^2 s^{-1}). The return pathway for AABW to the surface of the Southern Ocean is turned off. The total rate of AABW formation is decreased slightly (to 16 Sv from 20 Sv), The temperature of this bottom-forming water is reduced to -1°C to reflect the more extreme conditions in the Polar Southern Ocean.

The model tracks temperature (T), phosphate (P), alkalinity (A) and total dissolved inorganic carbon (C), modelling biological productivity and particle remineralisation by means of fixed Redfield ratios C(organic):P:C(inorganic) of 106:1:25. Particulate fluxes generated in the surface reservoirs are remineralised in the underlying boxes in fixed proportions (see Table 2). Atmospheric CO_2 is included as a reservoir, with pCO_2 calculated using a constant gas transfer velocity over the entire ocean surface. When required, carbonate compensation can be crudely simulated by restoring the carbonate concentration of the AABW reservoir to the value in the modern ocean, by adding or subtracting to the total A and C inventories in the ratio 2 : 1.

Table 3. Steady-state box model results

	1. Modern conditions	2. Glacial circulation, modern temperatures and Antarctic export production	3. As 2, but no Antarctic export production	4. As 2, but proxy-consistent Antarctic export production	5. As 4, but glacial temperatures (compare Figs 5e and 5f)	6. As 5, but adjust for 3% ocean volume change and 500 Pg terrestrial biosphere
Atmospheric pCO_2 (μatm)	280	245	269	232	208	249
Atmospheric pCO_2 after carbonate compensation (μatm)	280	223	253	211	187	210
Polar Antarctic surface PO_4 (μM)	1.9	1.07	1.53	1.15	1.15	1.15
Sub-Antarctic Surface PO_4 (μM)	1.1	0.37	0.76	0.30	0.30	0.30
Polar Antarctic export production (mol C m^{-2} yr^{-1})	1.20	1.29	0.05	0.56	0.56	0.56
Sub-Antarctic export production (mol C m^{-2} yr^{-1})	1.87	1.86	0.03	2.68	2.68	2.68

Table 3 collects the results of several experiments shifting between the modern day and glacial conditions. Column 1 gives the modern configuration. In column 2 we shift to the glacial circulation, keeping temperatures, inventories and particulate fluxes from the surface boxes constant. This results in a ∼35 ppm drawdown of atmospheric CO_2. If carbonate compensation is included, this increases to 57 ppm. The assumption of a constant particle flux is of course entirely *ad hoc*. Column 3 shows the result of setting export production in both the sub-Antarctic and Polar oceans almost to zero. In this case atmospheric CO_2 still decreases below the modern value, by some 27 ppm if carbonate compensation is included. Despite the cessation of biological activity, surface polar nutrient concentrations still decrease a little from modern values in this case. This is because the upwelling that brings nutrient-rich water to the surface is reduced, exposing the surface Polar ocean to eddy exchange with the near surface, relatively nutrient-poor water to the North.

In column 4, we apply export productivities to the sub-Antarctic and Polar Southern Ocean that are consistent with proxy data—polar export production is substantially reduced from the modern value but sub-Antarctic productivity is increased. The increase in the sub-Antarctic region can more than compensate for the decrease in the polar region in terms of the effect on atmospheric pCO_2. Column 5 reveals the effect of then imposing LGM surface temperatures (a further reduction of ∼25 ppm). Finally, in column 6 we account for two processes expected to increase atmospheric CO_2 in glacial time. These are the decrease in volume of the oceans due to build up of ice on land, which raises the carbon and phosphate concentrations and alkalinity, and the transfer of around 500 Pg of carbon from the oceans to the land as the terrestrial biosphere grew in biomass between the LGM and the present day. Final atmospheric concentrations are 70 ppm below the modern value in the case where carbonate compensation is allowed.

5. Conclusion

According to the ideas developed here, the modern deep ocean is relatively rapidly ventilated in the Southern Ocean by a combination of vigorous deep mixing and upwelling south of the Polar Front. In glacial time the mixing was slower because denser deep waters were formed and the decreased buoyancy flux at the surface suppressed upwelling. These changes serve to isolate the oceans deepest waters from the surface, allowing biologically fixed carbon to build up in them, removing it from the atmosphere and surface water, leading to reduction of atmospheric CO_2. In particular, the recognition of a direct connection between buoyancy flux and upwelling may be the key to understanding why atmospheric CO_2 is so closely tied to Antarctic temperatures, as shown in higher resolution records of the deglaciation from Antarctic ice cores (Monnin et al., 2001).

There is less direct evidence for the link postulated here between deep ocean mixing and CO_2. A reduction in deep mixing, if it occurred, would presumably have been a consequence of the lower temperatures leading to formation of deep water with more extreme properties. If it also contributed to lowering atmospheric CO_2, then it would have formed part of a self-reinforcing mechanism, with the resulting lower temperatures further suppressing the mixing, leading to yet lower CO_2. The same kind of positive feedback would also apply to the buoyancy reduction mechanism.

Recent hypotheses to explain the rise of CO_2 at the close of glacial time have focused on Antarctic processes. There seem to be three other versions in current discussion, and we end

by summarizing these and the predictions they make for the sequence of events at the termination.

(1) Stephens and Keeling (2000) focus on the 'capping' by Antarctic sea ice which slows down Southern Ocean ventilation by its effect on gas exchange. Because gas exchange is not normally a limiting factor in equilibrating the ocean with the atmosphere, this hypothesis requires a drastic reduction in gas exchange, implying that the ice coverage should be continuous and >90% for most of the year. Also, it should recede at the same time, or only slightly in advance of, the rise in atmospheric CO_2. If sea ice was not extensive in summer (Crosta et al., 1998a,b), this would be a fatal difficulty for this model. It has also been suggested that the wintertime ice receded 1–2 kyr in advance of the rise in CO_2 (Shemesh et al., 2002), although uncertainty is introduced by the cross-dating of ice core and sedimentary records.

(2) J. R. Toggweiler (personal communication) has recently suggested that the critical event was the northward movement of the wind belts, leading to reduced wind stress over the Southern Ocean and therefore reduced upwelling. This mechanism is in many respects similar in its effects to the change in heat flux that we have described, with the difference between them being the question of what physics is assumed to be important for the upwelling. Toggweiler assumes it is defined principally by wind stress, while we believe that in the glacial situation it would be determined by air–sea buoyancy flux.

There is currently no consensus about whether the wind stress was greater or less than today over the Southern Ocean during glacial time. Most atmospheric models and some interpretations of palaeo-data suggest stronger winds then (see Anderson and Archer, 2002, for a review of the subject). However, evidence for a southward shift of the wind belts at the last termination comes from the Chilean Lake District (McCulloch et al., 2000). This shift could be the primary cause of the CO_2 rise only if it occurred at the same time as, or up to a few hundred years before, the latter, so this hypothesis makes a firm prediction that may be tested by refining the dating of these events.

(3) Sigman and Boyle (2000) champion the hypothesis that increased stratification of the near-surface Southern Ocean was the main driver for CO_2 change, based largely on ^{15}N data that show more nutrient utilization in the region in glacial time (although new measurements cast doubt on these data, Robinson et al., 2004). From an ocean dynamics perspective, this idea has yet to be fully developed. Observations (Table 1) suggest that diapycnal mixing rates are already slow in the near-surface Southern Ocean today, while deep waters are not formed by open ocean deep convection but chiefly by shelf-ice interactions. In these circumstances, it is not clear why increasing near-surface stratification should have any effect on transport between the surface and underlying waters. As pointed out by Keeling and Visbeck (2001), it is the wind- and eddy-driven upwelling that brings deep water to the surface and this would if anything be enhanced by increased stratification, since the implied lower baroclinicity would lead to weaker eddy fluxes and, therefore, a stronger net residual mean circulation.

Although we are still some way from a consensus on the causes of the increase in atmospheric CO_2 at the terminations, the degree of convergence between these theories is encouraging. Furthermore, the hypotheses now under discussion are for the most part not mutually exclusive. They may rather be additive in their effects, so that a full explanation may involve a combination of them.

6. Acknowledgments

AJW acknowledges the NERC "GENIE" project (NER/I/S/2002/0217). A NERC postdoctoral fellowship (NER/I/S/2001/00727) supported ACNG during this work. We thank Robbie Toggweiler and an anonymous reviewer for helpful discussion and comments.

References

Adkins, J. F., McIntyre, K. and Schrag, D. P. 2002. The salinity, temperature, and delta O-18 of the glacial deep ocean. *Science* **298**, 1769–1773.

Anderson, D. M. and Archer, D. 2002. Glacial-interglacial stability of ocean pH inferred from foraminifera dissolution rates. *Nature* **416**, 70–73.

Archer, D., Winguth, A., Lea, D. and Mahowald, N. 2000a. What caused the glacial/interglacial atmospheric pCO_2 cycles? *Rev. Geophys.* **38**, 159–189.

Archer, D. E., Eshel, G., Winguth, A., Broecker, W., Pierrehumbert, R., Tobis, M. and Jacob, R. 2000b. Atmospheric pCO_2 sensitivity to the biological pump in the ocean. *Global Biogeochem. Cyc.* **14**, 1219–1230.

Bopp, L., Kohfeld, K. E., Le Queré, C. and Aumont, O. 2003. Dust impact on marine biota and atmospheric CO_2 during glacial periods. *Paleoceanogr.* **18**, art. no.-1046.

Broecker, W., Lynch-Stieglitz, J., Archer, D., Hofmann, M., Maier-Reimer, E., Marchal, O., Stocker, T. and Gruber, N. 1999. How strong is the Harvardton-Bear constraint? *Global Biogeochem. Cyc.* **13**, 817–820.

Bryden, H. L. and Cunningham, S. A. 2003. How wind-forcing and air-sea heat exchange determine the meridional temperature gradient and stratification for the Antarctic Circumpolar Current. *J. Geophys. Res. - Oceans* **108**, 10.1029,2001JC0011296.

Crosta, X., Pichon, J. J. and Burckle, L. H. 1998a. Application of modern analog technique to marine Antarctic diatoms: reconstruction of maximum sea-ice extent at the Last Glacial Maximum. *Paleoceanogr.* **13**, 284–297.

Crosta, X., Pichon, J. J. and Burckle, L. H. 1998b. Reappraisal of Antarctic seasonal sea ice at the Last Glacial Maximum, *Geophys. Res. Lett.* **25**, 2703–2706.

Egbert, G. D., Ray, R. D. and Bills, B. G. 2004. Numerical modeling of the global semidiurnal tide in the present day and in the last glacial maximum. *J. Geophys. Res.* **109**, C03003, doi: 10.1029/2003JC001973.

Ganachaud, A. and Wunsch, C. 2000. Improved estimates of global ocean circulation, heat transport and mixing from hydrographic data. *Nature* **408**, 453–457.

Gent, P. R., Large, W. G. and Bryan, F. O. 2001. What sets the mean transport through Drake Passage? *J. Geophys. Res. - Oceans* **106**, 2693–2712.

Gersonde, R. and Zielinski, U. 2000. The reconstruction of late Quaternary Antarctic sea ice distribution - the use of diatoms as a proxy for sea ice. *Paleogeogr., Paleoclim., Paleoecol.,* **162**, 263–286.

Gersonde, R., Crosta, X., Abelmann, A. and Armand, L. 2005. Sea surface termparature and sea ice distribution of the Southern Ocean at the EPILOG Last Glacial Maximum – a circum-Antarctic view based on siliceous microfossil records. *Quat. Sci. Rev.* **24**, 869–896.

Gill, A. E. 1982. *Atmosphere and ocean dynamics*. Cambridge University Press.

Goldson, L. E. 2004. Determining vertical mixing rates in the near-surface Southern Ocean using SF_6 releases. PhD thesis, School of Environmental Sciences, U. East Anglia.

Haine, T. W. N., Watson, A. J., Liddicoat, M. I. and Dickson, R. R. 1998. The flow of Antarctic bottom water to the southwest Indian Ocean estimated using CFCs. *J. Geophys. Res. - Oceans* **103**, 27637–27653.

Heywood, K. J., Naveira Garabato, A. C. and Stevens, D. P. 2002. High mixing rates in the abyssal Southern Ocean. *Nature* **415**, 1011–1014.

Karsten, R. H. and Marshall, J. 2002. Constructing the residual circulation of the ACC from observations. *J. Phys. Oceanogr.* **32**, 3315–3327.

Keeling, R. F. 2002. On the freshwater forcing of the thermohaline circulation in the limit of low diapycnal mixing. *J. Geophys. Res. - Oceans* **107**, 10.1029/2000JC000685.

Keeling, R. F. and Stephens, B. B. 2001. Antarctic sea ice and the control of Pleistocene climate instability. *Paleoceanogr.* **16**, 112–131.

Keeling, R. and Visbeck, M. 2001. Palaeoceanography - Antarctic stratification and glacial CO_2. *Nature* **412**, 605–606.

Knox, F. and McElroy, M. B. 1984. Changes in atmospheric CO_2 - Influence of the marine biota at high-latitude. *J. Geophys. Res. – Atmos.* **89**, 4629–4637.

Law, C. S., Abraham, E. R., Watson, A. J. and Liddicoat, M. I. 2003. Vertical eddy diffusion and nutrient supply to the surface mixed layer of the Antarctic Circumpolar Current. *J. Geophys. Res. - Oceans* **108**, 10.1029/2002JC001604.

Ledwell, J. R., Watson, A. J. and Law, C. S. 1998. Mixing of a tracer in the pycnocline. *J. Geophys. Res. - Oceans* **103**, 21 499–21 529.

Ledwell, J. R., Montgomery, E. T., Polzin, K. L., St. Laurent, L. C., Schmitt, R. W. and Toole, J. M. 2000. Evidence for enhanced mixing over rough topography in the abyssal ocean. *Nature* **403**, 179–182.

Mantyla, A. W. and Reid, J. L. 1983. Abyssal characteristics of the World Ocean waters. *Deep-Sea Res. A* **30**, 805–833.

Marshall, D. 1997. Subduction of water masses in an eddying ocean. *J. Mar. Res.* **55**, 201–222.

McCulloch, R. D., Bentley, M. J., Purves, R. S., Hulton, N. R. J., Sugden, D. E. and Clapperton, C. M. 2000. Climatic inferences from glacial and palaeoecological evidence at the last glacial termination, southern South America. *J. Quat. Sci.* **15**, 409–417.

Monnin, E., Indermuhle, A., Dallenbach, A., Fluckiger, J., Stauffer, B., Stocker, T. F., Raynaud, D. and Barnola, J. M. 2001. Atmospheric CO_2 concentrations over the last glacial termination. *Science* **291**, 112–114.

Munk, W. H. 1966. Abyssal recipes. *Deep-Sea Res.* **13**, 707–730.

Munk, W. and Wunsch, C. 1998. Abyssal recipes II: energetics of tidal and wind mixing. *Deep-Sea Res. I*, **45**, 1977–2010.

Naveira Garabato, A. C., Polzin, K. L., King, B. A., Heywood, K. J. and Visbeck, M. 2004. Widespread intense turbulent mixing in the Southern Ocean. *Science* **303**, 210–213.

Nilsson, J., Broström, G. and Walin, G. 2003. The thermohaline circulation and vertical mixing: does weaker density stratification give stronger overturning? *J. Phys. Oceanogr.* **33**, 2781–2795.

Nilsson, J., Broström, G. and Walin, G. 2004. On the spontaneous transition to asymmetric thermohaline circulation. *Tellus* **56A**, 68–78.

Olbers, D., Borowski, D., Völker, C. and Wolff, J.-O. 2004. The dynamical balance, circulation and transport of the Antarctic Circumpolar Current. *Antarct. Sci.* **16**, 439–470.

Orsi, A. H., Johnson, G. C. and Bullister, J. L. 1999. Circulation, mixing, and production of Antarctic Bottom Water. *Progr. Oceanogr.* **43**, 55–109.

Polzin, K. L., Toole, J. M., Ledwell, J. R. and Schmitt, R. W. 1997. Spatial variability of turbulent mixing in the abyssal ocean. *Science* **276**, 93–96.

Redi, M. 1982. Oceanic isopycnal mixing by co-ordinate rotation. *J. Phys. Oceanogr.* **12**, 1154–1157.

Rintoul, S. R. 1998. On the origin and influence of Adélie Land Bottom Water. In: *Ocean, ice and atmosphere: Interactions at the Antarctic continental margin*. Antarctic Research Series (eds. S. S. Jacobs and R. F. Weiss), 151–171.

Robinson, R. S., Brunelle, B. G. and Sigman, D. M. 2004. Revisiting nutrient utilization in the glacial Antarctic: evidence from a new method for diatom-bound N isotopic analysis. *Paleoceanogr.* **19**, 10.1029/2003PA000996.

Sarmiento, J. L. and Toggweiler, J. R. 1984. A new model for the role of the oceans in determining atmospheric pCO_2. *Nature* **308**, 621–624.

Shemesh, A., Hodell, D., Crosta, X., Kanfoush, S., Charles, C. and Guilderson, T. 2002. Sequence of events during the last deglaciation in Southern Ocean sediments and Antarctic ice cores. *Paleoceanogr.* **17**, 10.1029/2000PA000599.

Siegenthaler, U. and Wenk, T. 1984. Rapid atmospheric CO_2 variations and ocean circulation. *Nature* **308**, 624–626.

Sigman, D. M. and Boyle, E. A. 2000. Glacial/interglacial variations in atmospheric carbon dioxide. *Nature* **407**, 859–869.

Sloyan, B. M. and Rintoul, S. R. 2001. Circulation, renewal, and modification of Antarctic mode and intermediate water. *J. Phys. Oceanogr.* **31**, 1005–1030.

Speer, K., Guilyardi, E. and Madec, G. 2000. Southern Ocean transformation in a coupled model with and without eddy mass fluxes. *Tellus* **52A**, 554–565.

Stephens, B. B. and Keeling, R. F. 2000. The influence of Antarctic sea ice on glacial-interglacial CO_2 variations. *Nature* **404**, 171–174.

Talley, L. D. 1999. Some aspects of ocean heat transport by the shallow, intermediate and deep overturning circulations. In: *Mechanisms of global climate change at millenial time scales* (eds.P. U. Clark, R. S. Webb and L. D. Keigwin). American Geophysical Union, Washington DC, 1–22.

Toggweiler, J. R. 1999. Variation of atmospheric CO_2 by ventilation of the ocean's deepest water, *Paleoceanogr.* **14**, 571–588.

Toggweiler, J. R. and Samuels, B. 1995. Effect of Drake Passage on the global thermohaline circulation. *Deep-Sea Res. I* **42**, 477–500.

Toggweiler, J. R. and Samuels, B. 1998. On the ocean's large-scale circulation near the limit of no vertical mixing. *J. Phys. Oceanogr.* **28**, 1832–1852.

Toggweiler, J. R., Gnanadesikan, A., Carson, S., Murnane, R. and Sarmiento, J. L. 2003a. Representation of the carbon cycle in box models and GCMs: 1. Solubility pump. *Global Biogeochem. Cyc.* **17**, 10.1029/2001GB001401.

Toggweiler, J. R., Murnane, R., Carson, S., Gnanadesikan, A. and Sarmiento, J. L. 2003b. Representation of the carbon cycle in box models and GCMs - 2. Organic pump. *Global Biogeochem. Cyc.* **17**, 10.1029/2001GB001401.

Toole, J. M., Polzin, K. L. and Schmitt, R. W. 1994. Estimates of diapycnal mixing in the abyssal ocean. *Science* **264**, 1120–1123.

Walin, G. 1982. On the relation between sea-surface heat-flow and thermal circulation in the ocean. *Tellus* **34**, 187–195.

Watson, A. J., Bakker, D. C. E., Ridgwell, A. J., Boyd, P. W. and Law, C. S. 2000. Effect of iron supply on Southern Ocean CO_2 uptake and implications for glacial atmospheric CO_2. *Nature* **407**, 730–733.

Webb, D. J. and Suginohara, N. 2001. Oceanography - Vertical mixing in the ocean. *Nature* **409**, 37–37.

Whitworth, T., Nowlin, W. D., Orsi, A. H., Locarnini, R. A. and Smith, S. G. 1994. Weddell Sea Shelf Water in the Bransfield Strait and Weddell-Scotia Confluence. *Deep-Sea Res. I* **41**, 629–641.